JOURNAL OF MATERIALS SCIENCE 20 (1985) 1847–1858

Strain-induced transformation and plastic deformation behaviour of a 17Cr–7Ni–1Al steel at high hydrostatic pressure

YOSHINARI KAIEDA, ATSUSHI OGUCHI
Metal Processing Division, National Research Institute for Metals, 2-3-12 Nakameguro, Meguro-ku, Tokyo 153, Japan

Tensile tests of a 17Cr–7Ni–1Al steel were carried out at 0.1, 300 and 600 MPa hydrostatic pressure, and the mechanical properties of the material were found to be considerably changed by the pressure. The martensitic transition temperature $M_s^{\gamma \rightarrow \alpha'}$ decreased under pressure. The volume fraction of α-martensite induced by tensile deformation increased with strain, but was suppressed by hydrostatic pressure. The yield stress increased with pressure. The yield surface became a nonlinear cone with a pointed apex. The stress–strain curve was considerably changed by pressure, and was expressed by a modified identical-strain model (law of mixture) as a quantitative function. Uniform-strain limit increased with pressure. It was found that these changes were not caused by the mechanical effect of hydrostatic pressure, but by its thermodynamic effects.

1. Introduction

Modern plasticity theory is based on the experimental fact that the yielding of a metal is, to a first approximation, unaffected by a moderate hydrostatic pressure or tension [1, 2]. Theory also predicts that, as hydrostatic pressure has no effect on yielding behaviour, it should also have no effect on the form of the stress–strain curve and on the initiation of necking [3]. However, increase in ductility (reduction in area) after necking has been found in aluminium, copper, iron, Cu–Zn alloy, Cu–Ge alloy [4], magnesium, zinc, cobalt, tungsten and AISI 1045 steel [5], brasses [6, 7], free-machining brass [8], spheroidized 0.5% carbon steel [9], and aluminium alloy [10], because the initiation, growth and coalescence of voids were suppressed by high hydrostatic pressure. An increase in yield stress was also found in experiments on AISI 4310 and 4330 steels under high hydrostatic pressure [11], and a plastic analysis was carried out [12].

On the other hand, it was found that the stress–strain curve of material such as an 18–8 stainless steel, which exhibited strain-induced transformation, varied remarkably at various testing temperatures because the quantity of the strain-induced α-martensite (α'-phase) changed with temperature [13, 14]. Since the specific volume of the transformed α'-phase was different from that of the austenite (γ-phase) of the matrix, so that the $\gamma \rightarrow \alpha'$ transformation was expansile, a hydrostatic pressure might have suppressed the transformation and changed the stress–strain curve.

Nevertheless, in research on the influence of a high hydrostatic pressure on the flow stress of an 18–8 stainless steel [15], tensile tests were carried out at atmospheric pressure and a high hydrostatic pressure of 1.2 GPa, and the quantity of the strain-induced α'-phase was unaffected by pressure. The stress–strain curve at a hydrostatic pressure of 1.2 GPa exhibited only a monotonic stress increase by about 12% as a whole during overall strain, compared with that at atmospheric pressure. The above results were quite different from the results from the same sort of material obtained at various testing temperatures under atmospheric pressure [13, 14]. The difference between the

0022–2461/85 $03.00 + .12

influence of temperature and pressure resulted from the fact that ϵ-martensite (ϵ'-phase) was easily induced under a high hydrostatic pressure [15].

If experiments could be performed under conditions where the ϵ'-phase was not induced, the relationship between the stress–strain curve and the strain-induced α'-phase, and the influence of hydrostatic pressure on this relationship, would be clarified. A 17Cr–7Ni–1Al steel was found to be suitable for this condition. Tensile tests on this material were then carried out at atmospheric pressure, and at high hydrostatic pressures within the range over which the ϵ'-phase was not induced. The influence of hydrostatic pressure on the martensite transition temperature $M_s^{\gamma \rightarrow \alpha'}$, on the change in quantity of the strain-induced α'-phase, and on the change in the stress–strain curve, and the relationship among these phenomena, are reported in the present paper.

2. Materials and experimental procedure

2.1. Materials

The specimen used in the experiment was cold-drawn wire having a diameter of 1.1 mm. The chemical composition of the specimen was C: 0.088, Si: 0.47, Mn: 0.60, Cr: 17.15, Ni: 7.03, Al: 1.06 wt%, respectively. The specimens were annealed for 1.8 ksec at 1323 K and were water-quenched after being cut to the length of the test piece. These test pieces were called Specimens A. The remnants were kept at 1273 K (Specimens B), 1243 K (Specimens C), 1213, 1153, 1093 and 1033 K for 5.4 ksec in each case and water-quenched; these were used as test pieces for intermediate transformations. The mean crystal grain diameter was about 5 to 10 μm for Specimens A, B and C.

2.2. Tensile tests at high hydrostatic pressure

The apparatus for tensile tests at high pressure is described below only briefly, as it is fully reported elsewhere [16]. Unleaded gasoline was used as a pressure-transmitting medium. The tensile test could be carried out at any pressure up to the maximum of 1.5 GPa. However, the testing temperature could not be changed from the room temperature of 288 K. The gauge length of the test piece was 15 mm. The tensile speed was 8.3 μm sec^{-1}. The strain rate was 0.55×10^{-6} sec^{-1}. The tensile test was carried out at atmospheric pressure and at pressures of 300 and 600 MPa, for ϵ'-phase was not induced in the specimen at pressures up to 600 MPa.

2.3. Phases of specimens and measurements of $M_s^{\gamma \rightarrow \alpha'}$

The kind of phases that appeared in the specimen used in the present experiment after heat treatment and during tensile tests at atmospheric pressure and high hydrostatic pressure were austenite (γ-phase), δ-ferrite (δ-phase), α-martensite (α'-phase), and ϵ-martensite (ϵ'-phase) which was induced at a very high pressure above 900 MPa. The authentication of these phases and the measurement of the volume fraction of each phase were carried out by means of optical microscopy, X-ray diffraction and the measurement of magnetic properties. Incidentially, the γ-phase and ϵ'-phase were paramagnetic, while δ-phase and α'-phase were ferrogmagnetic.

The measurement of the volume fraction of the α'-phase that was induced during tensile deformation was carried out by means of a magnetic measurement. The coil used for the measurement had 300 turns of fine silk-covered wire of 0.08 mm diameter, The change in inductance (ΔL) of the coil, when the specimen was inserted into the coil, was measured by means of a Maxwell bridge. The current and frequency were 2.5 mA and 1.0 kHz.

The measurement of the temperature of $\gamma \rightarrow \alpha'$ transformation of the specimen was carried out only at atmospheric pressure, because the ambient temperature of the apparatus for the tensile test at a high pressure could not be changed. Dry ice and alcohol were used as a freezing mixture. The initiation of the generation of α'-phase was examined by the magnetic measurement.

3. Experimental results

3.1. Crystal structures and lattice constants

The observation of the microstructure by optical microscopy and X-ray diffraction were carried out on the annealed Specimen A and the other six kinds of intermediate-transformation specimens including Specimens B and C. The three kinds of Specimens A, B and C were found to consist of γ-phase for the most part, and of a small quantity of δ-phase. However, a considerable amount of α'-phase was observed in the other four kinds of intermediate-transformation specimen. No differ-

TABLE I Crystal structure and lattice constant measured by X-ray diffraction*

Phase†	Structure	Lattice constants (nm)
γ	FCC	$a = 0.3594$
δ	BCC	$a = 0.2876$
α'	BCT	$a = 0.2876$, $c/a \simeq 1.0$
ϵ'	HCP	$a = 0.2534$, $c = 0.4132$, $c/a = 1.63$

†$\Delta V^{\gamma \to \alpha'} = +0.1737\ \mathrm{cm^3\ mol^{-1}}$, $\Delta V^{\gamma \to \epsilon'} = -0.093\,12\ \mathrm{cm^3\ mol^{-1}}$

*Cobalt target, K_α wavelength 0.1790 nm; iron filter

ences in the optical-microscopic microstructure were found among Specimens A, B and C. No ϵ'-phase was observed in any of the seven kinds of specimen.

The crystal structures and lattice constants measured with X-ray diffraction are shown in Table I. The measured values of the lattice constants of the ϵ'-phase were obtained at the initial stage of the tensile test at very high pressure above 900 MPa, and will be mentioned later. The values of the volume change of $\gamma \to \alpha'$ and $\gamma \to \epsilon'$ transformations obtained by calculation of the measured values of the lattice constants are also shown in Table I. The $\gamma \to \alpha'$ transformation is expansile and the $\gamma \to \epsilon'$ transformation is contractile.

3.2. Magnetic properties and $M_s^{\gamma \to \alpha'}$

The inductance of the measuring coil was changed in the case of the annealed specimens and the intermediate-transformation specimens. The results of the measurements of magnetic properties are shown in Fig. 1. At least ten samples were tested for each kind of specimen. Little scatter was found in the measured values. A small amount of magnetic property remains in Specimens A, B and C as shown in Fig. 1. Optical microscopy and X-ray diffraction revealed that this magnetic property was caused by δ-phase. The magnetic properties of the four kinds of specimen which had been heat treated below 1213 K increased remarkably with decrease of the treatment temperature. The reason for this is that transformation from γ-phase to α'-phase occurred, because the $M_s^{\gamma \to \alpha'}$ temperature was raised above room temperature by the intermediate-transformation treatment. The volume fraction of the δ-phase was not changed by this treatment.

Quantitative magnetic measurement of the α'-phase was performed by the following procedure. The specimen which was heat-treated at 1033 K and contained the most α'-phase was cooled to liquid nitrogen temperature, and was subjected to tensile deformation at room temperature. In this way the residual γ-phase was transformed to the α'-phase as much as possible. X-ray diffraction measurement revealed that the specimen had no residual γ-phase. The magnetic intensity (corrected for the reduction in area) of the above specimen was taken to be the magnetic intensity of a specimen with 100% α'-phase. The volume fractions of the α'-phase in other specimens were calculated on the basis of this magnetic intensity. However, the specimen had a small amount of δ-phase as stated above, and did not exactly have 100% α'-phase. The magnetic intensity per unit volume of the δ-phase is almost

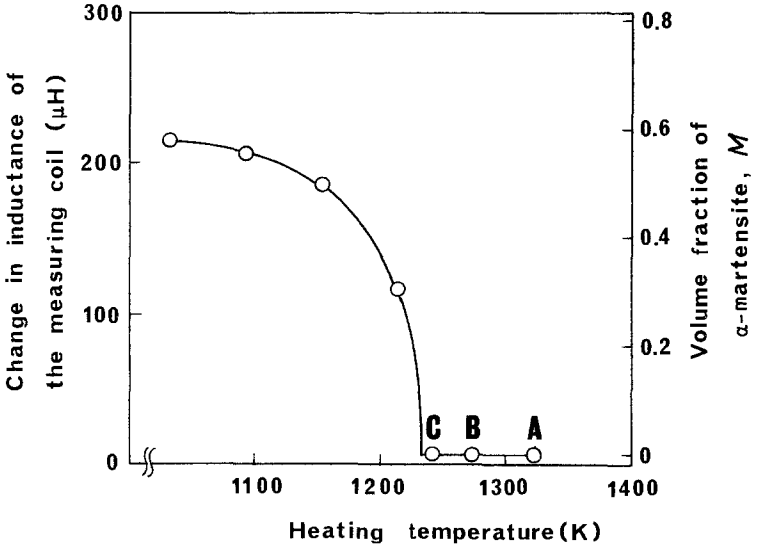

Figure 1 Variation of inductance of measuring coil and volume fraction of α-martensite with heat-treatment temperature.

TABLE II Martensitic transition temperatures $M_s^{\gamma\rightarrow\alpha'}$ (K)

Pressure (MPa)	0.1	300	600
Specimen A	229	205*	176*
Specimen B	258	236*	214*
Specimen C	278	258*	235*

*Obtained from Fig. 4.

the same as that of the α'-phase [17], and the volume fraction of the δ-phase included in Specimens A, B and C was estimated at 2% of a whole specimen. The magnetic intensity of the δ-phase was therefore subtracted from the whole magnetic intensity, and the remainder exhibited as a volume fraction of α'-phase on the vertical axis of the right side in Fig. 1. Quantitative measurement of the α'-phase by means of this method was used in all the following discussions. Three kinds of specimens (A, B and C) out of seven kinds were suitable for the purpose of the present investigation, because these three specimens contained no α'-phase before the tensile test. The results on these three Specimens A, B and C are discussed below, but the results on the other specimens are not discussed.

The results of the measurement of the transition temperature $M_s^{\gamma\rightarrow\alpha'}$ for Specimens A, B and C at atmospheric pressure are shown in the column headed 0.1 MPa in Table II. Values of $M_s^{\gamma\rightarrow\alpha'}$ obtained in this study were almost the same as those obtained by Krauss *et al.* [18] on the same kinds of material.

3.3. Strain-induced transformation

Tensile tests on Specimens A, B and C were carried out at 0.1, 300 and 600 MPa of hydrostatic pressure. The change in the volume fraction of strain-induced α'-phase, M, is plotted against the strain (true strain) during the tensile test in Fig. 2. The numbers and letters in Fig. 2 represent the experimental pressure (MPa) and the kind of specimens. At least ten specimens were tested for each experimental condition. The scattering of results under each condition was very small. The mean value of the measured volume fraction of α'-phase under each set of conditions is plotted in Fig. 2.

3.4. Yield stress

The macroscopic yield stress, σ_y, of each kind of specimen obtained from the stress–strain curve at each pressure is shown in Table III. The numerical values listed are averaged from at least ten specimens tested at each pressure. There is little variation of the values from specimen to specimen. It is obvious that the yield stress of each specimen increases steeply and nonlinearly with increasing hydrostatic pressure.

3.5. Stress–strain curves

Stress–strain curves (the plastic-flow curves of true stress and true strain, $\sigma-\epsilon$ curves) were obtained from the same specimens used for the measurement of the volume fraction of strain-induced α'-phase as in Fig. 2; they are shown as solid lines in Fig. 3. The curves are displaced in origin (in the same order as the curves shown in Fig. 2) to avoid confusion. The numbers and letters represent the intensity of pressure and the kind of the specimen, respectively. The end of each curve corresponds to the starting-point of necking or the limit of uniform strain.

Fig. 3 shows that the uniform-strain limit of each specimen increased with increase of environmental pressure under tensile testing. Comparing the uniform-strain regions of the three kinds of specimen tested at the same pressure, the uniform-strain limit of Specimen A is larger than that of Specimen C.

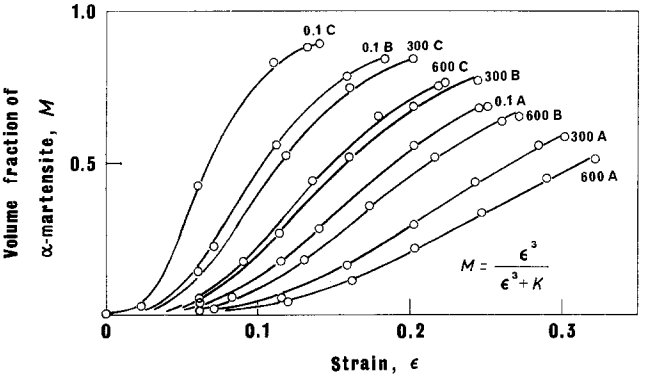

Figure 2 Changes in volume fraction of α-martensite with strain.

TABLE III Yield stresses and material constants of yield function

Yield stress, σ_y (MPa)				Material constants of yield function*		
Pressure (MPa)	0.1	300	600	α_0	α_1	α_2
Specimen A	295	351	366	184.29	−0.04250	-1.650×10^{-5}
Specimen B	274	342	363	174.10	−0.05273	-1.951×10^{-5}
Specimen C	261	337	347	168.60	−0.06149	-2.729×10^{-5}

*Yield function: $J_2^{1/2} = \alpha_0 + \alpha_1 I_1 + \alpha_2 I_1^2$

4. Discussion

4.1. Change in $M_s^{\gamma \to \alpha'}$ caused by intermediate-transformation treatment

The values of $M_s^{\gamma \to \alpha'}$ for Specimens B and C were different from that of Specimen A. This is explained as follows [17, 18]: $M_{23}C_6$ (where M = metal), a carbide of chromium, was slightly precipitated in the γ-phase during the intermediate-transformation treatment, and dissolved carbon and chromium, which had the effect of decreasing $M_s^{\gamma \to \alpha'}$, decreased in the γ-phase so that the γ-phase became more unstable and resulted in a rise of $M_s^{\gamma \to \alpha'}$. Therefore, Specimens A, B and C not only had different values of $M_s^{\gamma \to \alpha'}$, but might have different mechanical properties because Specimens B and C might have been affected by the effect of the precipitation-hardening of $M_{23}C_6$. However, Yukawa *et al.* [17, 19] observed microstructure of the same kind as in the present material by transmission electron microscopy, and concluded that precipitates of $M_{23}C_6$ during intermediate-transformation treatment were very few; they could hardly have caused precipitation hardening, though they made the γ-phase unstable and raised $M_s^{\gamma \to \alpha'}$. Consequently, we were able to make a comparison between the stress–strain curves of Specimens A, B and C, assuming that differences were caused only by differences in $M_s^{\gamma \to \alpha'}$, even though they were differently heat-treated.

4.2. Changes in $M_s^{\gamma \to \alpha'}$ caused by hydrostatic pressure

Since the $\gamma \to \alpha'$ transformation is expansile, the transformation is suppressed by a high hydrostatic pressure and $M_s^{\gamma \to \alpha'}$ decreases. $M_s^{\gamma \to \alpha'}$ could not be measured directly by changing the testing temperature in the present high-pressure testing apparatus. Accordingly, the change in $M_s^{\gamma \to \alpha'}$ caused by hydrostatic pressure was calculated by using the thermodynamic quantities and lattice constants shown in Table I.

The thermodynamic equation involving the effects of the chemical composition of the material, derived by Kaufman *et al.* [20, 21], was used to calculate $M_s^{\gamma \to \alpha'}$ in the present study. The difference in free energy during the $\gamma \to \alpha'$ transformation under a hydrostatic pressure $\Delta F^{\gamma \to \alpha'}$ is expressed by

$$\Delta F^{\gamma \to \alpha'}(x, y, T, P) = \Delta F^{\gamma \to \alpha'}(x, y, T) + P \Delta V^{\gamma \to \alpha'}(x, y) \quad (1)$$

where x and y represent the atomic fraction of nickel and chromium and T and P represent temperature and hydrostatic pressure, while ΔV represents the volume change in the transformation. The first term on the right hand side of Equation 1 represents the chemical energy, while the second term represents the mechanical energy. Equation 1 reduces to

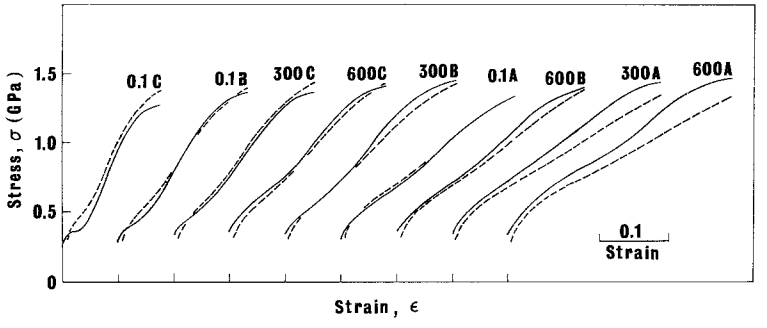

Figure 3 Stress–strain curves at various pressures (solid lines) and predicted stress–strain curves (broken lines).

$$\Delta F^{\gamma\rightarrow\alpha'}(x,y,T,P) = -4.184\{(1-x-y) \times (1202-2.63\times10^{-3}T^2 + 1.54\times10^{-6}T^3) + y(460+T) + X(-3700 + 7.09\times10^{-4}T^2 + 3.91\times10^{-7}T^3) + y(1-x-y)(-2800+0.75T) + x(1-x-y)[3600+0.58T(1-\ln T)]\} + P\Delta V^{\gamma\rightarrow\alpha'} \text{ J mol}^{-1} \quad (2)$$

where the coefficient 4.184 is the coefficient of conversion from calories to Joules. Although the effects of nickel and chromium as main alloying elements were considered in Equation 2, it was necessary to compensate the equation for the effects of secondary elements such as aluminium, carbon etc. Compensation was accomplished by adding terms like $w\Delta H^{\gamma\rightarrow\alpha'}$ to the right hand side of Equation 2, according to Kaufman and Cohen [22]; w is the atomic fraction of each secondary element, while $\Delta H^{\gamma\rightarrow\alpha'}$ is the difference between the heats of solution of each element in the γ-phase and in the α'-phase. The value of $\Delta H^{\gamma\rightarrow\alpha'}$ for each element is as follows: carbon $+3.4\times10^4$, silicon -2.0×10^3, manganese $+1.1\times10^4$, aluminium -5.4×10^3 J mol^{-1} [22].

Equation 2 was calculated by using the value of the change in volume obtained from the lattice constants shown in Table I and the results of chemical analysis of the present material, and was compensated for the effects of small amounts of elements such as aluminium and carbon. The value of $\Delta F^{\gamma\rightarrow\alpha'}$ was then obtained at atmospheric pressure, 300 and 600 MPa, respectively. The results are shown in Fig. 4. The difference in free energy necessary for the $\gamma\rightarrow\alpha'$ transformation of Specimen A at atmospheric pressure is obtained from Fig. 4 as $\Delta F^{\gamma\rightarrow\alpha'} = -1.87$ kJ mol^{-1}, because $M_s^{\gamma\rightarrow\alpha'}$ for the specimen is 229 K at atmospheric pressure. Since transformation under high pressure is considered to occur at the same value of the difference in free energy as at atmospheric pressure, $M_s^{\gamma\rightarrow\alpha'}$ is obtained at 205 K at 300 MPa and 176 K at 600 MPa; the results from Fig. 4 are shown in Table II. $M_s^{\gamma\rightarrow\alpha'}$ for Specimens B and C under high hydrostatic pressure are obtained by the same procedure in for specimen A, and are also shown in Table II. The change in $M_s^{\gamma\rightarrow\alpha'}$, $dM_s^{\gamma\rightarrow\alpha'}/dP$, caused by hydrostatic pressure is then about -70 to -100 deg (GPa)$^{-1}$. This value is comparable to experimental values of

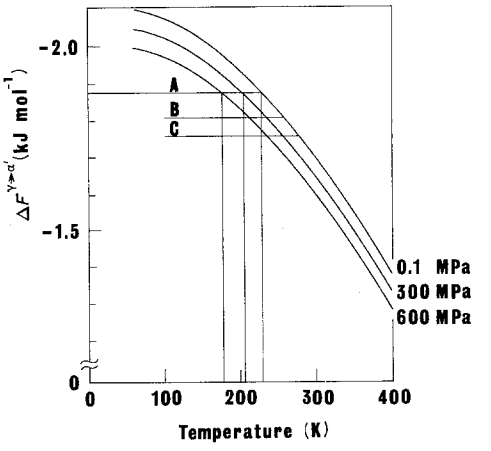

Figure 4 Difference in free energy necessary for $\gamma\rightarrow\alpha'$ transformation.

$-75\sim-83$ deg (GPa)$^{-1}$ obtained by Fisher and Turnbull [23] and Patel and Cohen [24] in steel and 70Fe–30Ni alloys.

4.3. Strain-induced transformation caused by tensile deformation

Deformation induces a $\gamma\rightarrow\alpha'$ transformation, called strain-induced transformation, in the temperature range above $M_s^{\gamma\rightarrow\alpha'}$ and below M_d (the maximum temperature at which the $\gamma\rightarrow\alpha'$ transformation can be induced). In this temperature range, the lower the experimental temperature, the more the degree of strain-induced transformation. In the case of the present study, every experiment was carried out at the temperature of the pressure-transmitting medium (288 K). However, the $M_s^{\gamma\rightarrow\alpha'}$ was changed by intermediate heat-treatment and by hydrostatic pressure. Experimental results were therefore classified by the temperature difference, ΔT, between the experimental temperature and the value of $M_s^{\gamma\rightarrow\alpha'}$ shown in Table II.

In Fig. 2, the volume fraction of the transformed α'-phase of Specimens A, B and C at the same strain decreases with increasing pressure, because the $\gamma\rightarrow\alpha'$ transformation, which is expansile, is suppressed under higher pressures. Comparing the three kinds of specimen at three pressures, we see that the lower value of $M_s^{\gamma\rightarrow\alpha'}$, (Table II), that is to say the larger the temperature difference ΔT, the less the volume fraction of transformed α'-phase at the same strain. However, observation of the microstructure of the specimen by optical microscopy revealed that the volume fraction of δ-phase was unchanged by the applica-

tion of pressure and by tensile tests under pressures up to 600 MPa. The reason was that the experimental temperature was low and the δ-phase was thermodynamically stable.

The same kind of experiment was carried out at higher pressures, namely at 900 MPa and 1.2 GPa. A small amount of ϵ'-phase appeared at the initial stage of the tensile deformation, through $\gamma \rightarrow \epsilon'$ transformation. It was observed that in response to this phenomenon the stress–strain curve rose at the initial stage of the test. The ϵ'-phase disappeared through $\epsilon' \rightarrow \alpha'$ transformation with increasing deformation, so that it was not observed by the middle stage of the deformation. The lattice constants of the ϵ'-phase, obtained by X-ray diffraction of a specimen for which the tensile test was discontinued at the initial stage of deformation, are shown in Table I. Analyses of the results of tensile tests under these higher pressures were omitted from the present paper, because they were not relevant to its purpose.

There are two reasons for the occurrence of the $\gamma \rightarrow \alpha'$ transformation induced by deformation temperatures higher than $M_s^{\gamma \rightarrow \alpha'}$. One reason is that the tensile stress acting as a hydrostatic tension changes the sign of the second term of Equation 1, and opposes the decrease of $M_s^{\gamma \rightarrow \alpha'}$ shown in Fig. 4 so that $M_s^{\gamma \rightarrow \alpha'}$ is raised. Another is that the shear stress promotes martensitic transformation because the transformation occurs as a form of shear deformation. The external work necessary for the $\gamma \rightarrow \alpha'$ transformation, U, was given by Patel and Cohen [24] as

$$U = \tau\gamma_0 + \sigma\epsilon_0$$
$$= \tfrac{1}{2}\left[\gamma_0\sigma_t \sin 2\theta \pm \epsilon_0\sigma_t(1 + \cos 2\theta)\right] \quad (3)$$

where τ and σ are shear stress and tensile stress acting on the habit plane respectively; ϵ_0 and γ_0 are expansile volume strain and shear strain, θ is the angle between the tensile axis and the normal to the habit plane, and σ_t is the applied tensile stress. In Equation 3 the maximum value, U_{max}, is obtained when

$$\tan 2\theta = \pm\gamma_0/\epsilon_0 \quad (4)$$

The lattice constants shown in Table I were used for the calculation by matrix algebra analysis of the martensitic transformation according to Bowles–Mackenzie theory [25], and the following values were obtained:

$$\begin{aligned} \epsilon_0 &= 0.02486 \\ \gamma_0 &= 0.2247 \\ \gamma_0/\epsilon_0 &= 9.041 \\ \theta &= 0.73 \text{ rad } (U = U_{max}) \end{aligned} \quad (5)$$

The rate of increase of U_{max} due to external tensile stress was obtained from the above values as

$$dU_{max}/d\sigma_t = 0.883 \text{ J(mol MPa)}^{-1} \quad (6)$$

On the other hand, from the relation between the difference in chemical free energy $\Delta F^{\gamma \rightarrow \alpha'}$ and the temperature shown in Fig. 4, we obtain

$$d\Delta F^{\gamma \rightarrow \alpha'}/dT = +2.1 \text{ J(mol deg)}^{-1} \quad (7)$$

Therefore, the rate of increase of $M_s^{\gamma \rightarrow \alpha'}$ due to external tensile stress becomes

$$\begin{aligned} dM_s^{\gamma \rightarrow \alpha'}/d\sigma &= (dU_{max}/d\sigma_t)/(d\Delta F^{\gamma \rightarrow \alpha'}/dT) \\ &= 0.42 \text{ deg MPa}^{-1} \end{aligned} \quad (8)$$

Consequently, as $M_s^{\gamma \rightarrow \alpha'}$ shown in Table II is higher, the $\gamma \rightarrow \alpha'$ transformation is induced more easily.

When a martensitic crystal is initiated during a tensile deformation, a stress field is created near the crystal by its deformation. The stress field promotes the initiation of another new martensitic crystal. In other words, transformation is promoted by an auto-catalytic effect [26]. Consequently, the volume fraction of the α'-martensite, M, should be the function of the strain ϵ. As an empirical equation for M as shown in Fig. 2 we obtained

$$M = \epsilon^3/(\epsilon^3 + K). \quad (9)$$

where K is a constant. The solid lines in Fig. 2 are drawn by using Equation 9, for which K was obtained by the least-squares method. The linear relationship between the constant K and $\Delta T/M_s^{\gamma \rightarrow \alpha'}$ is shown in the logarithmic plot of Fig. 5. This relationship is expressed by the empirical equation

$$\begin{aligned} K &= 0.1\,(\Delta T/Ms^{\gamma \rightarrow \alpha'})^2 \\ &= 0.1\,[\Delta T/(288 - \Delta T)]^2. \end{aligned} \quad (10)$$

Equation 9 is then rearranged to give

$$M = \epsilon^3/\{\epsilon^3 + 0.1\,[\Delta T/(288 - \Delta T)]^2\}. \quad (11)$$

Equation 11 shows that the volume fraction of the strain-induced α'-phase, M, may be expressed as a function of strain, ϵ, and ΔT which is the difference between the experimental temperature and $M_s^{\gamma \rightarrow \alpha'}$.

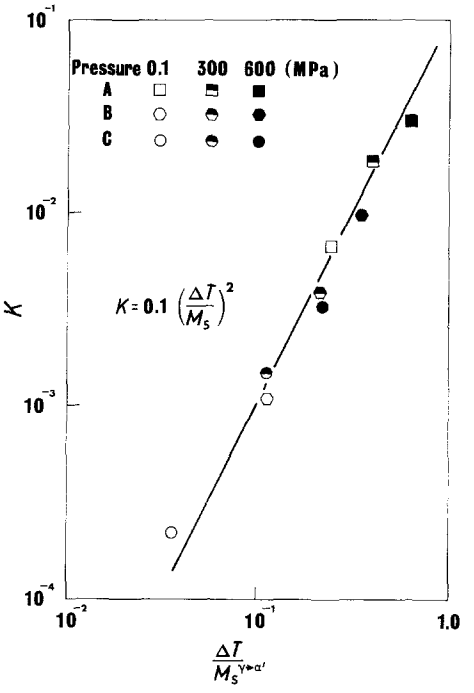

Figure 5 Constant K (Equation 9) against $\Delta T/M_s^{\gamma\to\alpha'}$.

4.4. Change in yield stress caused by hydrostatic pressure

In general, the yield stress of metals increases at high hydrostatic pressures. However, compared with many polymers the degree of increase in yield stress of many metals is small, and is not more than 2.0% per 700 MPa of hydrostatic pressure [27], though Spitzig *et al.* [11] obtained values of 4.8% and 3.7% per 700 MPa as the increase in yield stress under high hydrostatic pressure from experiments on AISI 4310 and 4330 steels, respectively. As compared with this fact, the increase in yield stress of the present material is remarkably large. Moreover, in contrast with many other materials [11, 27], the yield stress of the present material increased nonlinearly.

This increase in yield stress of the present material caused by hydrostatic pressure can be explained qualitatively as follows. α'-phase is certainly induced to a small degree when the tensile test is at the initial stage (including the elastic zone and the initial plastic zone where plastic strain is almost zero). In this case the volume of expansion due to $\gamma \to \alpha'$ transformation is not negligible, as compared with the amount of strain due to deformation. This expansion results in stress-relaxation. The volume fraction of the initiated α'-phase near zero strain is not clear from Fig. 2. However, as in the case of large strain, $\gamma \to \alpha'$ transformation must be active at low pressures, and this stress relaxation effect should be large. At high pressures, the stress relaxation effect becomes less, because $\gamma \to \alpha'$ transformation is suppressed. Therefore, with increasing pressure, macroscopic yield stress apparently increases much higher than with usual metallic materials.

This change in yield stress due to pressure may also be approached from the point of view of the theory of plasticity. From this viewpoint, whether the material is a metal [12] or a polymer [28], the yield condition is of the form

$$f(I_1, J_2^{1/2}) = 0 \tag{12}$$

and

$$J_2^{1/2} = \sum_{i=0}^{N} \alpha_i (I_1)^i \tag{13}$$

where I_1 is the first invariant of the stress tensor, J_2 is the second invariant of the deviatoric stress tensor, and α_i is the material constant. I_1 and J_2 are expressed as follows:

$$I_1 = \sigma_1 + \sigma_2 + \sigma_3 \tag{14}$$

$$J_2 = [(\sigma_1 - \sigma_2)^2 + (\sigma_2 - \sigma_3)^2 + (\sigma_3 - \sigma_1)^2]/6 \tag{15}$$

where σ_1, σ_2 and σ_3 are principal normal stresses. Equation 13 may be reduced to various forms depending on the value of N [28]. If $N = 0$, it reduces to von Mises' yield criterion

$$J_2 = \alpha_0^2 \tag{16}$$

If the yield stress increases linearly with pressure, as obtained on AISI 4310 and 4330 steels [11] and polyoxymethylene [28], it is expressed by the following equation [12, 28],

$$J_2^{1/2} = \alpha_0 + \alpha_1 I_1 \qquad (N = 1) \tag{17}$$

If the yield stress increases nonlinearly against pressure as obtained with polypropylene, it is expressed by

$$J_2^{1/2} = \alpha_0 + \alpha_1 I_1 + \alpha_2 I_2^2 \qquad (N = 2) \tag{18}$$

Though the present material is a metal, the behaviour of the change in yield stress due to hydrostatic pressure is expressed exactly by Equation 18 because the change in yield stress is nonlinear. The values of α_1, α_2 and α_3 were calculated by the least-squares method to fit the values of yield stress in Table III, and are also given there. As a representative of the three kinds of specimen, the

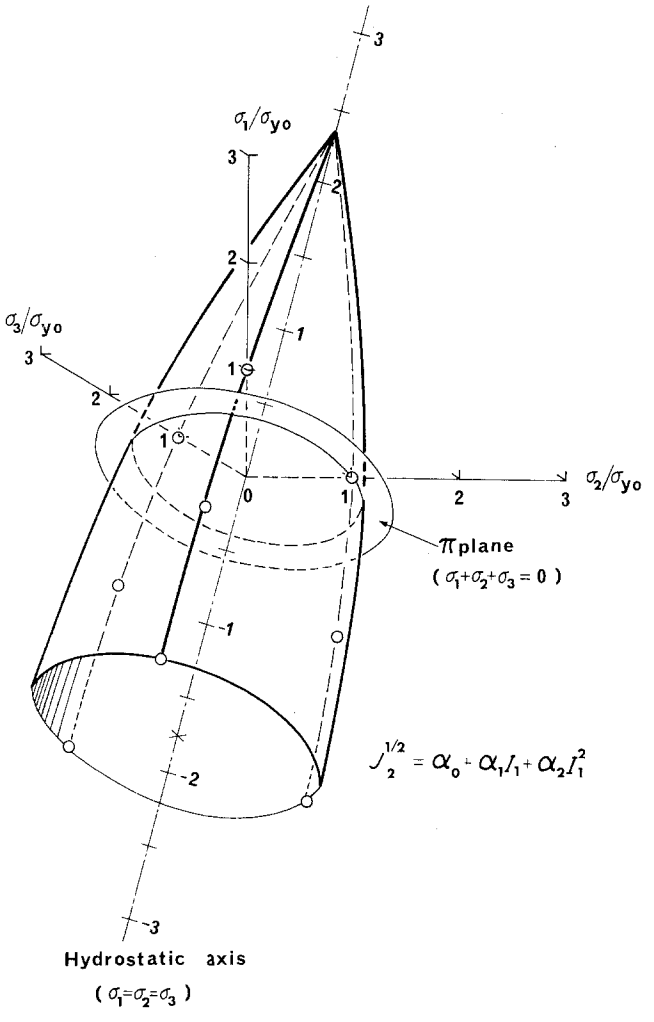

Figure 6 Yield surface of specimen *B*.

yield surface of Specimen B calculated from Equation 18 is shown in three principal stress coordinates in Fig. 6. In Fig. 6, three principal stresses are normalized by being divided by the yield stress at atmospheric pressure, σ_{y0}. The yield surface is a nonlinear cone with a pointed apex at the hydrostatic axis. The small circles represent experimental data, and the solid line represents the theoretical prediction. Yield surfaces similar to that of Specimen B were obtained for Specimens A and C.

The crystal structure and the bonding forces in a metal are quite different from those of a polymer. In the case of the polymer, the yield stress changes under hydrostatic pressure because Young's modulus changes considerably at high pressures [29]. However, the increase in yield stress of the present material under pressure is caused by the transformation expansion. Though the physical meaning of the cause of the increase is different from that of the polymer case, the changes in yield stress of both materials are phenomenologically analogous, so that they are expressed by the same form of equation from the viewpoint of plasticity theory.

4.5. Change in stress–strain curve caused by hydrostatic pressure

The shape of any $\sigma-\epsilon$ curve after yielding (Fig. 3) was mainly decided by the balance of the strain hardening of the γ phase (whose volume fraction decreases with strain) and of the α'-phase (whose volume fraction increases with strain), and the stress-relaxation due to the expansion associated with $\gamma \rightarrow \alpha'$ transformation. This balance was changing continuously with strain, so that the $\sigma-\epsilon$ curve adopted a peculiar shape in which two points of inflection appeared between the yielding point and the starting point of necking. Since the shape of the $\sigma-\epsilon$ curve was strongly affected by

the volume fraction of transformed α'-phase, the shapes of the nine σ–ϵ curves shown in Fig. 3 were closely related to those of the volume fraction of the transformed α'-phase of each specimen against strain as shown in Fig. 2, namely to the temperature $M_s^{\gamma\rightarrow\alpha'}$ which was determined by the kind of specimen and the testing pressure. The serrations which sometimes appear in the σ–ϵ curve with strain-induced $\gamma \rightarrow \alpha'$ transformation were not observed in the present experiments, because the grain size was small compared with the diameter of the specimen.

The σ–ϵ curves shown in Fig. 3 were considered to be affected secondarily by the strength of the δ-phase and by the mechanical effect of hydrostatic pressure. However, the volume fraction of the δ-phase was no more than 2.0% and was considered to contribute about 2.0% to the overall strength. The mechanical effect of 700 MPa of pressure on the strength of many metallic materials has been reported to be about 2.0% [27]. These two secondary effects on the σ–ϵ curves were therefore negligibly small in the present study.

Attempts have been made to express these σ–ϵ curves as quantitative functions, and the predicted σ–ϵ curves calculated from the functions compared with the experimental curves. In general, it is difficult to express the σ–ϵ curve of a dual-phase alloy with a function. However, Ludwigson and Berger [30] tried to express the σ–ϵ curve of materials in which the $\gamma \rightarrow \alpha'$ transformation occurs as functions of strain and volume fraction of transformed α'-phase. They proposed the following expression;

$$\sigma = A\epsilon^B(1-M) + CM^D \qquad (19)$$

where A, B, C and D are material constants. In the present study, as mathematical models for the form of the function and the roles of γ- and α'-phase, we used the Ludwigson model [30]; the identical-strain model (law of mixture) assuming that the strain of γ- and α'-phases were the same; the identical-stress model assuming that the stress of γ-phase and α'-phase was the same; an intermediate between identical-strain and identical-stress models, and so forth. After many trials and calculations we found the following equation which was as simple as possible and agreed well with the experimental σ–ϵ curve;

$$\sigma = R_\gamma \epsilon_\gamma^{n(\gamma)}(1-M) + R_{\alpha'}\epsilon_{\alpha'}^{n(\alpha')}M \qquad (20)$$

where R_γ, $n(\gamma)$ for the γ-phase and $R_{\alpha'}$, $n(\alpha')$ for the α'-phase are material constants common to three kinds of specimen under all pressures; ϵ_γ and $\epsilon_{\alpha'}$ are the strains of γ- and α'-phases, respectively. We found

$$\begin{aligned} R_\gamma &= 144 \\ n(\gamma) &= 0.3 \\ R_{\alpha'} &= 180 \\ n(\alpha') &= 0.1 \\ \epsilon_\gamma &= \epsilon \\ \epsilon_0 &= 0.02486 \\ \epsilon_{\alpha'} &= \epsilon - \epsilon_0/3 = \epsilon - 0.0082 \end{aligned} \qquad (21)$$

M is given by Equation 11. Equation 20 is a modified equation for an identical-strain model (law of mixture). In the equation, the strain of the γ-phase was considered to be the same as the strain of the specimen, and the strain lag of the α'-phase due to dilatation by the transformation was considered. $\epsilon_0/3$ is a linear expansion due to the transformation. The numerical value of ϵ_0 is obtained from Equation 5. In Equation 20 the volume fraction, the strength and the strain hardening of γ- and α'-phases, and the stress-relaxation due to transformation with expansion are considered. The σ–ϵ curves calculated from Equation 20 are shown as broken lines in Fig. 3. These theoretical predictions do not strictly agree with the experimental curves, for Equation 20 is based on the above-mentioned hypothesis and disregards small factors. However, the qualitative σ–ϵ relations of the present materials under three kinds of pressure can be roughly expressed by Equation 20.

4.6. Change in uniform-strain limit caused by hydrostatic pressure

In general, changes in the uniform-strain limit of normal single-phase metals and alloys due to hydrostatic pressure are scarcely observable. The great increase in ductility of the present material due to pressure is considered to be influenced by the change with strain of the volume fraction of transformed α'-phase (Fig. 2). The change in uniform-strain limit due to pressure exhibited in the present study is considered to be essentially the same as transformation-induced plasticity, which occurs when the strain-induced transforming material is deformed between temperatures $M_s^{\gamma\rightarrow\alpha'}$ and M_d. However, in the present experi-

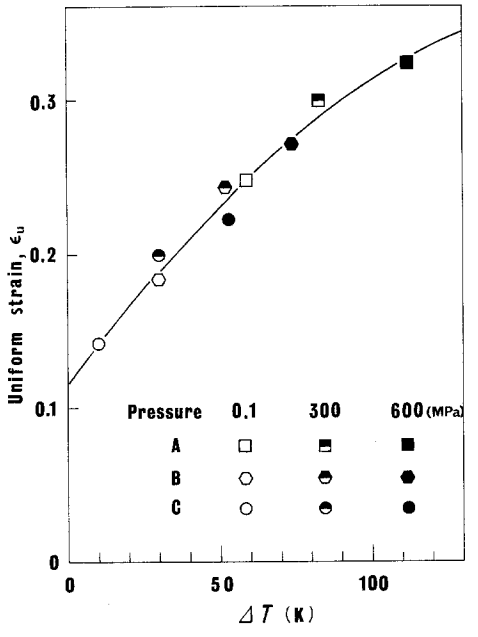

Figure 7 Uniform-strain limit against ΔT.

ments the experimental temperature was constant (288 K) but $M_s^{\gamma\to\alpha'}$ was changed. Consequently, the uniform strain (true strain) is plotted against the temperature difference between $M_s^{\gamma\to\alpha'}$ (Table II) and the experimental temperature, as shown in Fig. 7. As shown in Fig. 7, the uniform strain ϵ_u increases against ΔT independently of the kind of specimen within the experimental pressure range. The relationship between ϵ_u and ΔT is expressed by the following equation and is shown by the solid line in Fig. 7;

$$\epsilon_u = 1.16 \times 10^{-1} + 2.67 \times 10^{-3}\,\Delta T - 7.06 \times 10^{-6}\,\Delta T^2 \quad (22)$$

Incidentally, the uniform strain of a normal material is given by

$$d\sigma/d\epsilon = \sigma \quad (23)$$

because the volume of the specimen is constant during a tensile test. However, the relationship of Equation 23 cannot be used in the present study because the material undergoes a volume change during the $\gamma \to \alpha'$ transformation. In addition, in the usual transformation-induced plasticity the maximum ductility lies midway between $M_s^{\gamma\to\alpha'}$ and M_d, and the ductility decreases near $M_s^{\gamma\to\alpha'}$ and M_d. From this point of view, in Fig. 7, a maximum ϵ_u should be exhibited if ΔT increases, and after this point ϵ_u should decrease with increasing ΔT.

5. Conclusions

In general, the mechanical properties of normal metallic materials such as yield stress, stress–strain curve and uniform strain are scarcely affected by hydrostatic pressure. In the present study, however, tensile tests of a 17Cr–7Ni–1Al steel, which was a strain-induced transforming material, were carried out under three pressures, (0.1, 300 and 600 MPa) and the mechanical properties of the material were found to be changed by hydrostatic pressure. The main results obtained are as follows:

1. Three kinds of specimen which had the same microstructure but different values of $M_s^{\gamma\to\alpha'}$ could be made by appropriate heat treatment. $M_s^{\gamma\to\alpha'}$ decreased under pressure for all specimens. The amount of the decrease was about -70 to -100 deg GPa^{-1}.

2. The volume fraction of α-martensite (α'-phase) induced by tensile deformation increased with strain ϵ, but was suppressed by hydrostatic pressure. It could be expressed as a function of strain ϵ and the temperature difference ΔT between the experimental temperature and $M_s^{\gamma\to\alpha'}$, which was determined by the heat treatment and the magnitude of the pressure.

3. Yield stress increased under hydrostatic pressure, because under high pressure the transformation from austenite (γ-phase) to α'-phase ($\gamma \to \alpha'$ transformation) was suppressed, and the amount of stress-relaxation due to the expansion of transformation decreased. The relationship between yield stress and hydrostatic pressure was expressed by the yield function proposed by Pae [28]. The yield surface became a nonlinear cone with a pointed apex.

4. The stress–strain curve was changed considerably by hydrostatic pressure. As a result of the suppression of $\gamma \to \alpha'$ transformation by high pressure, the slope of the stress–strain curve became moderate, and the uniform-strain limit increased. The remarkable change in the stress–strain curve owing to the pressure was correlated roughly with the volume fraction of γ-phase and transforming α'-phase, the strength and the strain hardening of both phases, and the stress-relaxation by expansion of the $\gamma \to \alpha'$ phase transformation. Taking these factors into consideration, the stress–strain curve was expressed by a modified identical-strain model (law of mixture) as a quantitative function.

5. The uniform strain limit, which gave an index of the ductility of the specimen, increased

with increasing pressure. The increase in uniform-strain limit resulted from transformation-induced plasticity. In the pressure range of the present experiments, the increase was related to an increase in the temperature difference, ΔT, between the $M_s^{\gamma \to \alpha'}$ and the experimental temperature.

The above-mentioned results were not caused by the direct mechanical effect of hydrostatic pressure on the deformation of the materials. The main cause was that $M_s^{\gamma \to \alpha'}$ decreased at high pressures, because the chemical free energy difference of the $\gamma \to \alpha'$ transformation was added to the mechanical energy term, which was the product of the specific volume change of the transformation and the pressure. In other words, these results were caused by the thermodynamic effect of a hydrostatic pressure.

References

1. P. W. BRIDGMAN, *Rev. Mod. Phys.* **17** (1945) 3.
2. R. HILL, "The Mathematical Theory of Plasticity" (Clarendon Press, Oxford, 1960) p. 16.
3. J. M. ALEXANDER, *J. Inst. Metals* **93** (1965) 366.
4. M. YAJIMA, M. ISHII and M. KOBAYASHI, *Int. J. Fract. Mech.* **6** (1970) 139.
5. T. E. DAVIDSON, J. C. UY and A. P. LEE, *Acta Metall.* **14** (1966) 937.
6. I. E. FRENCH and P. F. WEINRICH, *Scr. Metall.* **8** (1974) 7.
7. *Idem, Acta Metall.* **21** (1973) 1533.
8. I. E. FRENCH, P. F. WEINRICH and C. W. WEAVER, *ibid.* **21** (1973) 1045.
9. I. E. FRENCH and P. F. WEINRICH *Scr. Metall.* **8** (1974) 87.
10. *Idem, J. Aust. Inst. Metall.* **22** (1977) 40.
11. W. A. SPITZIG, R. J. SOBER and O. RICHMOND, *Acta Metall.* **23** (1975) 885.
12. Y. M. GUPTA, *ibid.* **25** (1977) 1509.
13. G. J. GUNTNER and R. P. REED, *Trans. ASM* **55** (1962) 399.
14. H. C. FIEDLER, B. L. AVERBACH and M. COHEN, *ibid.* **47** (1955) 267.
15. A. OGUCHI and S. YOSHIDA, *Trans. Jpn Inst. Met.* **14** (1973) 314.
16. S. YOSHIDA and A. OGUCHI, *Trans. Nat. Res. Ins. Met. (Jpn.)* **11** (1969) 347.
17. N. YUKAWA, M. MIZUTANI and H. SAKA, *J. Jpn Inst. Met.* **31** (1967) 850.
18. G. KRAUSS and B. L. AVERBACH, *Trans. ASM* **52** (1960) 434.
19. N. YUKAWA, M. MIZUTANI and H. SAKA, *J. Jpn Inst. Met.* **31** (1967) 855.
20. L. KAUFMAN, *Trans. AIME* **215** (1959) 218.
21. L. KAUFMAN, A. LEYENAAR and J. S. HARVEY, "Progress in Very High Pressure Research", edited by F. P. Bundy, W. R. Hibbard, Jr. and H. M. Strong (Wiley, New York 1961) p. 90.
22. L. KAUFMAN and M. COHEN, "Progress in Metal Physics 7", edited by B. Chalmers and R. King (Pergamon, London, 1958) p. 165.
23. F. C. FISHER and D. TURNBULL, *Acta Metall.* **1** (1953) 310.
24. J. R. PATEL and M. COHEN, *ibid.* **1** (1953) 531.
25. C. M. WAYMAN, "Introduction to the Crystallography of Martensitic Transformations" (Macmillan, New York, 1964) p. 112.
26. E. S. MACHLIN and M. COHEN, *Trans. AIME* **191** (1951) 746.
27. J. O. CHUA and A. RUOFF, *J. Appl. Phys.* **46** (1975) 4659.
28. K. D. PAE, *J. Mater. Sci.* **12** (1977) 1209.
29. Y. KAIEDA and K. D. PAE, *ibid.* **17** (1982) 369.
30. D. C. LUDWIGSON and J. A. BERGER, *J. Iron and Steel Inst.* **207** (1969) 63.

Received 30 April
and accepted 26 July 1984